Electric Power Systems Research 241 (2025) 111408

Contents lists available at ScienceDirect

Electric Power Systems Research

journal homepage: www.elsevier.com/locate/epsr

Enhancement of power quality based on dynamic voltage restorer matrix inverter-sliding mode control scheme

Abdul Hameed Soomro [a], Abdul Sattar Larik [b], Mukhtiar Ahmed Mahar [b], Anwer Ali Sahito [b], Mohsin Ali Koondhar [a], Yun-Su Kim [c,*], Zuhair Muhammed Alaas [d], Ezzeddine Touti [e], M.M.R. Ahmed [f]

[a] Department of Electrical Engineering, Quaid-e-Awam University of Engineering, Science and Technology, Sindh 67480 Pakistan
[b] Department of Electrical Engineering, Mehran University of Engineering and Technology Jamshoro, Pakistan
[c] Graduate School of Energy Convergence, Gwangju Institute of Science and Technology (GIST), Gwangju 61005, South Korea
[d] Department of Electrical and Electronics Engineering, Faculty of Engineering and Computer Science, Jazan University, Jizan 45142, Saudi Arabia
[e] Center for Scientific Research and Entrepreneurship, Northern Border University, Arar 73213, Saudi Arabia
[f] Faculty of Technology and Education, Helwan University, Cairo, Egypt

ARTICLE INFO

Keywords:
Voltage sag
Matrix converter
Dynamic voltage restorers
Sliding Mode Controller

ABSTRACT

This paper introduces a novel application of a three-phase matrix converter for Dynamic Voltage Restorers (DVRs), which is capable of direct AC-AC power conversion without the need for an energy storage component. Motivated by the need for efficient and responsive voltage sag correction, a sliding mode controller (SMC) with a Proportional-Integral (PI) sliding surface and hysteresis control is proposed. To optimize the PI gains of the SMC, traditional methods such as the real-coded genetic algorithm were considered; however, these methods typically involve extended convergence times. The Ant Colony Optimization (ACO) technique was employed, resulting in optimal PI gains of 6.87688 and 0.850851. The effectiveness of the SMC was validated under conditions of faults and load variations demonstrating satisfactory performance and stabilization at the onset of voltage sags. Numerical analysis reveals that the SMC maintains a THD % of 2.24 % adhering to the IEEE standard 519–1992. The DVR's performance, empowered by the matrix converter with the SMC framework, has been thoroughly analyzed, and the THD % was further scrutinized using the Fast Fourier Transform. This research confirms the matrix converter integrated with SMC as a robust solution for dynamic voltage restoration, providing a promising avenue for enhancing power quality in modern distribution networks.

1. Introduction

The distribution system is the part of the power system that provides electricity to residential, commercial, and industrial consumers. In recent days, every consumer has desired to receive disturbance-free voltage for the proper operation of their sensitive loads [1]. Voltage sag is the decrease in voltage from 10 % to 90 % of normal supply voltage [2] and commonly occurs in the distribution system, which inadequately affects the performance of sensitive loads [3]. Researchers have presented voltage sag compensation devices such as Static Var Compensator (SVC), Static Compensator (STATCOM), and Distribution Static Compensator (DSTATCOM), but these devices involve a high cost of installation and maintenance, and they can only alleviate low levels of voltage sag [4]. The essential components of a conventional DVR are an energy storage device, a filter, and a voltage source inverter (VSI) [5,6]. A DVR based on VSI requires an energy storage unit, resulting in complexity, high installation, and maintenance costs, and a need for more energy to alleviate high-value voltage sags [3,7]. This research paper proposes a three-phase matrix converter consisting of 09 bidirectional Insulated Gate Bipolar Transistor (IGBT) switches connected in such a way that they form a matrix [8]. Currently, a commercially available single device capable of conducting current in both directions and blocking voltage in either direction has not yet been developed [9]. Nevertheless, some research has focused on the monolithic bidirectional switch and various bidirectional IGBT structures [10]. The matrix converter has the capability of direct AC-AC power conversion and does not require an energy storage device, resulting in less complexity, lower installation and maintenance costs of DVR topology, and direct power

* Correspondence author.
E-mail address: yunsukim@gist.ac.kr (Y.-S. Kim).

https://doi.org/10.1016/j.epsr.2025.111408
Received 9 April 2024; Received in revised form 25 December 2024; Accepted 3 January 2025
Available online 8 January 2025

intake from the source [11,12]. The switching operation of the three-phase matrix converter consists of four possible groups based on 27 switching states [13].

In each state, only one switch will operate in each phase, and the other switches remain off to prevent short circuits [9]. The SMC is nonlinear and commonly used to control the nonlinearities in system parameters[14]. The implementation of SMC has been suggested as a means to ensure the reliable performance of the DVR under conditions of fault occurrence or load changes and is designed with a PI sliding surface and hysteresis control [15]. It is essential to select the best optimization technique to obtain the optimum parameters for the PI sliding surface [7]. The optimum parameters of PI gains are obtained by researchers through different methods, such as the Ziegler-Nichols method, but it takes more time, and sometimes, they obtained parameters result in a large overshoot [16]. According to previous studies, the Real Coded Genetic Algorithm has a longer convergence time compared to other optimization techniques, such as the PSO method, which has been reported to be less reliable in certain scenarios [17]. In this research paper, the Ant Colony Optimization technique (ACO) is presented to obtain the optimum values of PI gains [18–20]. The ACO technique requires less computational time, offers greater stability, and has smaller uncertainties than other optimization techniques [21]. In conventional DVRs, the VSI is commonly used to convert DC into AC, so it requires an energy storage device and charge-up circuit [22]. In this study, we have analyzed the system under 5 kW load, so the installation cost of VSI for DVR is 1.8Million because it requires batteries and a charge-up circuit, which leads to an increase in the installation and maintenance cost [23, 24] and also DVR with VSI compensate the low value of voltage sag [22]. PID controller is a linear controller and fails to perform under parameter variations [3–5].

The scope of this research extends to exploring the synergy between a matrix converter-based DVR and SMC, presenting a pioneering approach to power quality enhancement [25–27]. This combination is anticipated to address the quick response needs of sensitive loads and contribute to the robustness and reliability of the power distribution network[28,29]. The novel application and performance metrics of this integrated solution set a new precedent in the field, potentially revolutionizing the landscape of voltage sag mitigation and power quality improvement[30,31].

The pursuit of advancements in power distribution systems has led to the development of this research, which centers on mitigating voltage sags through a novel Dynamic Voltage Restorer (DVR) design[32–34]. Traditional DVR systems, while effective to a degree, are encumbered by the necessity of energy storage devices and are often limited to mitigating low-level voltage sags. This study propels the DVR [28–31] concept forward by integrating a three-phase matrix converter that sidesteps the need for such storage solutions, leading to a more streamlined, cost-effective, and efficient design[35,36]. The matrix converter stands as a testament to innovation in power electronics, offering a direct AC-AC power conversion and a reduction in complexity and expenses[37,38]. In conjunction with the matrix converter, this paper highlights the employment of a Sliding Mode Controller (SMC) [32] with a PI sliding surface for enhanced control during voltage sags. This approach showcases an improvement in performance, especially in scenarios involving load variations and fault conditions[39].

Our contribution is thus distilled into the following key points:

- **Matrix Converter Integration**: By incorporating a matrix converter, this research advances a DVR system that operates without an energy storage device, leading to a simplification in DVR topology that promises lower installation and maintenance costs.
- **Performance under Load Variations**: The SMC's performance has been meticulously assessed through load variations to validate its capability to provide an optimal DVR topology that ensures reduced costs and enhanced performance during voltage sags.
- **SMC Implementation**: The proposed SMC, designed with a PI sliding surface and hysteresis control, demonstrates an ability to maintain DVR performance amidst system nonlinearities and parameter changes, ensuring reliable power quality enhancement.
- **Optimization Technique Application**: The introduction of the Ant Colony Optimization (ACO) technique for determining optimal PI gain values represents an improvement over traditional methods, with benefits including reduced computational time and enhanced system stability.
- **Empirical Validation**: Through MATLAB Simulation Software, the study provides empirical evidence of the SMC's capability to control voltage sag scenarios efficiently, ensuring compliance with established IEEE standards for Total Harmonic Distortion (THD).
- **Cost-Efficiency Analysis**: The research delves into the economic implications of the proposed system, demonstrating the potential for significant cost savings in both the installation and maintenance of DVR systems.

2. Literature review

The DVR is valueless without a control circuit. Researchers presented the different control approaches to control the dynamics of DVR such as [40] proposed a novel control strategy based on the Uncertainty and Disturbance Estimator (UDE) for enhancing the response of the DVR in compensating load voltage under various power quality issues, specifically those related to grid voltage disturbances. Their approach utilizes the VSI, which requires multiple conversions and an energy storage device, resulting in increased costs for the DVR topology. In [41] presented a control strategy using SMC to regulate the dynamics of the DVR, incorporating an AC chopper. However, it was noted that the AC chopper is not suitable for output frequency control like a matrix converter. In [3] conducted an analysis of the DVR's performance using both PI and SMC controllers in conjunction with a VSI. It has been observed that the utilization of VSI requires multiple conversions and an energy storage device, resulting in increased costs for the DVR topology employing either PI or SMC. In [42] developed an enhanced synchronous reference frame (ESRF) theory-based DVR using a VSI with a PI controller to mitigate the effects of voltage sags. It has been observed that the utilization of VSI requires multiple conversions and an energy storage device, resulting in increased costs for the DVR topology, and it was found that the linear PI controller's performance was unsatisfactory under parameter variations. In [7] presented a control strategy for the DVR using SMC, incorporating PSO to optimize the tuning parameters of the PI controller for improved robustness. However, they also pointed out that the VSI necessitates multiple conversions and energy storage devices, thereby increasing the installation and maintenance costs of the proposed DVR topology. In [43] introduced a control strategy based on SMC for managing the dynamics of the DVR, utilizing a VSI. It has been observed that the converter circuit requires multiple conversions and energy storage devices, leading to elevated costs associated with the installation and maintenance of the proposed DVR topology. In [22] implemented a Voltage Source Converter (VSC) with an energy storage system and employed a PI controller to regulate the dynamics of the DVR. They found that the linear PI controller's performance was unsatisfactory under parameter variations. Additionally, the VSI necessitates an energy storage unit and charge-up circuit, resulting in high installation and maintenance costs for the DVR topology. In [44] presented the control strategy based on the half-cycle averaging method under steady-state conditions and selected the multi-stage converter, phase angle regulator, and tap-changing transformer, but this topology increases the complexity, installation, and maintenance costs, and DVR cannot operate satisfactorily under the fault condition. In [45] presented the PI controller with VSI and employed the photovoltaic (PV) system, but at nighttime, the PV cell will not generate power, and the PI controller is linear and fails to perform satisfactorily under parameter variations. In [46] presented the control strategy of a

Proportional-Integral-Derivative (PID) controller with a single-phase matrix converter to analyze the DVR performance under fault conditions. A matrix converter is a good approach, but PID is a linear controller and gives unsatisfactory performance under fault conditions.

The survey of existing literature reveals a significant research gap in the domain of Dynamic Voltage Restorer (DVR) control strategies. While various approaches have been explored to enhance DVR performance, there remains a clear opportunity to refine these systems' efficiency, cost-effectiveness, and adaptability under diverse electrical disturbances. The related work underscores a reliance on traditional methods, which involve multiple power conversions and necessitate additional components, leading to increased complexity and costs. This gap is addressed in our study by proposing an innovative DVR topology that leverages a matrix converter and an advanced control strategy.

Key gaps identified from the literature include:

- **Dependence on Complex Systems**: Current strategies often require complex systems like VSI with multiple energy conversions, leading to increased cost and complexity in DVR topology [43].
- **Inadequate Control Strategies:** Existing control strategies, including linear controllers like PI and PID, have shown unsatisfactory performance under parameter variations and fault conditions [42].
- **Energy Storage Dependency**: Many DVR topologies are dependent on energy storage devices, which contribute to elevated costs and maintenance requirements [18,22,24].
- **Suboptimal Parameter Optimization**: Approaches such as PSO have been used for tuning controller parameters but still lack robustness compared to potential alternatives like the Ant Colony Optimization technique [7].
- **Cost-Effective SMC Integration**: While SMC offers a promising control strategy for DVR systems, its application within a VSI context has not adequately addressed the cost concerns associated with traditional DVR topologies [8–9].
- **Untapped Potential of Matrix Converters**: There is a notable absence in the literature of research that combines the advantageous features of matrix converters with the robustness of SMC for DVR applications.
- **Limited Performance Under Variations**: Despite various advancements, there is still a need for a control strategy that can satisfactorily perform under different load and fault conditions without the need for additional energy storage [44].

Our research aims to bridge these gaps by introducing a simplified DVR system that reduces the installation and operational costs while maintaining high performance in voltage sag mitigation.

3. Dynamic voltage restorer

DVR is a series-connected device that adds the necessary voltage to the load during the small or high value of voltage sag [47]. Under steady-state conditions, the DVR remains in standstill condition but comes in voltage injection mode during voltage sag, and necessary voltage will be added to the load [22]. Fig. 1 shows the DVR with a distribution system. The compensation of voltage is given in Eq. (1) [15].

$$V_{load}(t) = V_{source}(t) + V_{DVR}(t) \tag{1}$$

Where,

$V_{source}(t)$ is the Supply voltage before compensation. $V_{load}(t)$ is the load voltage and $V_{DVR}(t)$ is the voltage injected by DVR. The load power in each phase is given in Eq. (2),

$$S_{load} = V_{load} I_{load} = P_{lpad} - jQ_{load} \tag{2}$$

Where,

$I_{load,}$ V_{load} are the load current and load voltage.

P_{load}, jQ_{load} are the active and reactive components consumed by the load, so the power of the load is given in Eq. (3),

$$S_{load} = (P_{load} - jQ_{load}) + (P_{DVR} - jQ_{DVR}) \tag{3}$$

The Proposed topology of DVR consists of SMC, a three-phase matrix converter, an LC filter, and three single-phase voltage injection transformers, as shown in Fig. 2 [1]. The distribution system consists of 11Kv grid voltage, which is supplied to the distribution transformer of 50 KVA (delta/star) for step-down of the voltage to 400 V, which is supplied to the RL load of 5KW with line impedance of RL. The DVR consists of three-phase direct matrix converters with an SVPWM switching technique, which converts three-phase AC to AC voltage directly without the support of an energy storage unit [13]. The SMC consists of PI with hysteresis control to control the dynamics of DVR under voltage sag [15]. IGBT switches are available in the matrix converter. An LC filter is utilized to compensate the harmonics [1]. Three voltage injection transformers of 1:1 were utilized to compensate the voltage in each phase individually [8]. The By-pass switches were utilized to isolate the DVR under normal conditions and connected with DVR under voltage sag [48].

3.1. Three-Phase matrix converter

The three-phase matrix converter consists of 09 bidirectional IGBT switches [49,50] and is capable of converting AC-AC voltage directly without an energy storage device and charge-up circuit [51,52], which will result in less installation and maintenance costs of DVR topology. Fig. 3 shows the three-phase direct matrix converter; in each phase, three IGBT switches with filter are connected [53]. The commutation

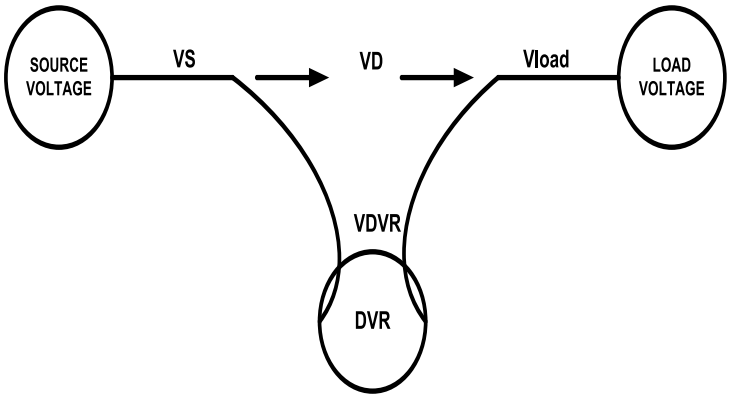

Fig. 1. Distribution system network with DVR.

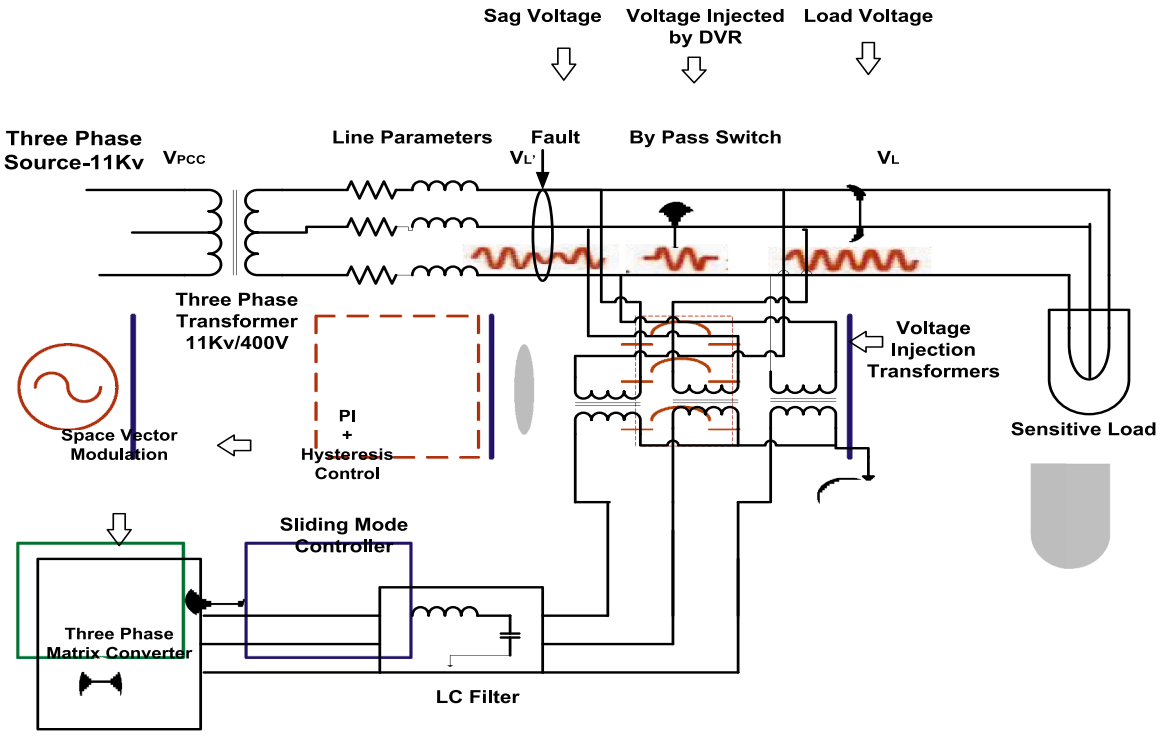

Fig. 2. Proposed DVR Topology.

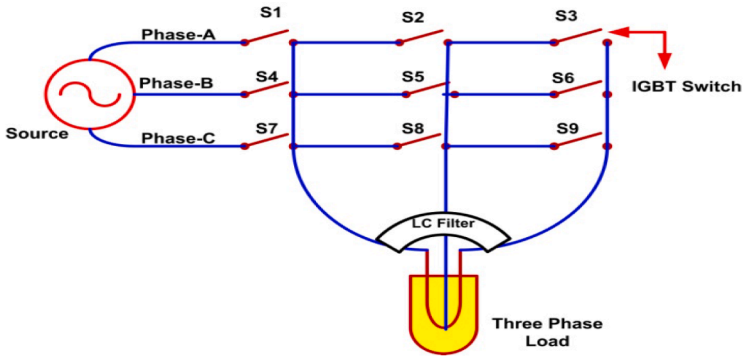

Fig. 3. Three-phase direct matrix converter.

will be achieved through the proper connection of IGBT switches, i.e., input parameters must be connected with output parameters [54]. Matrix converter can generate the best current signals with a convenient power factor and take the power from the same power source [51,55]. Protection of IGBT switches is essential against over current and over voltage [49]. The diode bridge with an electrolyte capacitor can be utilized for the protection of IGBT switches [56]. The switching states of the three-phase matrix converter are given in Table 1 [57].

The input phases must not be short-circuited, and the output phases must not be open-circuited. A single switch is allowed to operate in each phase during one switching state; otherwise, a short circuit will occur [58]. The current commutation is essential for IGBT switches for the safe transfer of current from one switch to another switch [59,60]. The simulation model of the three-phase matrix converter is shown in Fig. 4 [61], and output voltages with and without LC filter are shown in Figs. 5 (a) and 5(b) [49].

The relationship between load and source voltages [62] is given in Eq. (4)

$$\begin{bmatrix} V_a^{(t)} \\ V_b^{(t)} \\ V_c^{(t)} \end{bmatrix} = \begin{bmatrix} S_{Aa}^{(t)} & S_{Ba}^{(t)} & S_{Ca}^{(t)} \\ S_{Ab}^{(t)} & S_{Bb}^{(t)} & S_{Cb}^{(t)} \\ S_{Ac}^{(t)} & S_{Bc}^{(t)} & S_{Cc}^{(t)} \end{bmatrix} \begin{bmatrix} V_A^{(t)} \\ V_B^{(t)} \\ V_C^{(t)} \end{bmatrix} \tag{4}$$

$$V_o = T.V_i \tag{5}$$

Where T denotes the matrix converter transfer function, the output and input currents relationship is given in Eq. (6).

Table 1
Switching states of three-phase matrix converter.

State	Phase			Switching Function								
	R	Y	B	SAR	SAY	SAB	SBR	SBY	SBB	SCR	SCY	SCB
1	R	Y	B	√	×	×	×	√	×	×	×	√
2	R	B	Y	√	×	×	×	×	√	×	√	×
3	Y	R	B	×	√	×	√	×	×	×	×	√
4	Y	B	R	×	√	×	×	×	√	√	×	×
5	B	R	R	×	×	√	√	×	×	√	×	×
6	B	Y	R	×	×	√		√	×	√	×	×
7	R	B	B	√	×	×	×	×	√	×	×	√
8	R	B	B	×	√	×	×	×	√	×	×	√
9	Y	R	R	×	√	×	√	×	×	√	×	×
10	B	R	R	×	×	√	√	×	×	√	×	×
11	B	Y	Y	×	×	√	×	√	×	×	√	×
12	R	R	Y	√	×	×	√	×	×	×	√	×
13	B	R	B	×	×	√	√	×	×	×	×	√
14	B	Y	B	×	×	√	×	√	×	×	×	√
15	R	B	R	√	×	×	×	√	×	√	×	×
16	R	B	R	√	×	×	×	×	√	√	×	×
17	Y	B	R	×	√	×	×	×	√	×	√	×
18	Y	R	Y	×	√	×	√	×	×	×	√	×
19	B	B	R	×	×	√	×	×	√	√	×	×
20	B	B	Y	×	×	√	×	×	√	×	√	×
21	R	R	Y	√	×	×	√	×	×	×	√	×
22	R	R	B	√	×	×	√	×	×	×	×	√
23	Y	Y	B	×	√	×	×	√	×	×	×	√
24	Y	Y	R	×	√	×	×	√	×	√	×	×
25	R	R	R	√	×	×	√	×	×	√	×	×
26	Y	Y	Y	×	√	×	×	√	×	×	√	×
27	B	B	B	×	×	√	×	×	√	×	×	√

Where √ denotes the ON condition and × denotes the OFF condition of the IGBT switch, and R, Y, and B are the three phases of the matrix converter.

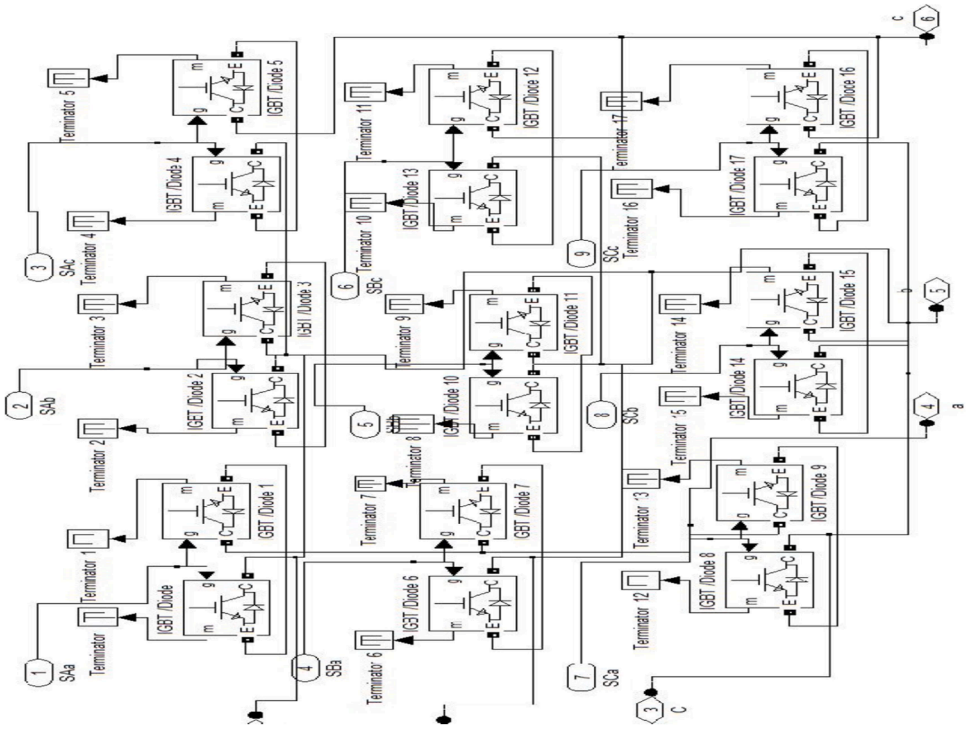

Fig. 4. Simulation model of three-phase matrix converter.

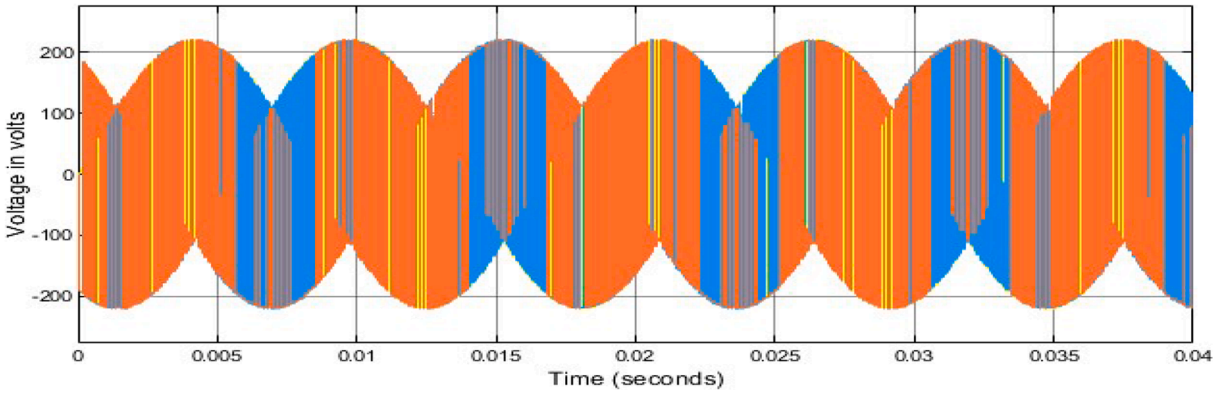

Fig. 5a. Output voltage of matrix converter.

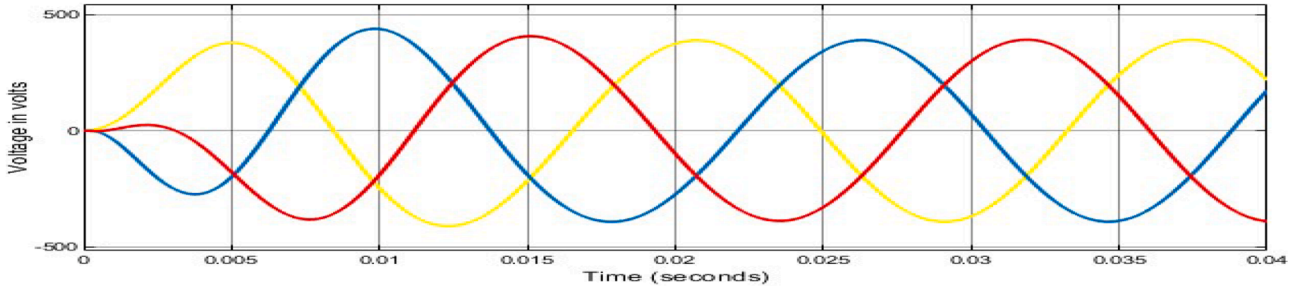

Fig. 5b. Output voltage of three phase matrix converter with LC filter.

$$i_i = \begin{bmatrix} i_a^{(t)} \\ i_b^{(t)} \\ i_c^{(t)} \end{bmatrix} i_o = \begin{bmatrix} i_A^{(t)} \\ i_B^{(t)} \\ i_C^{(t)} \end{bmatrix} \tag{6}$$

$$i_i = T^T . i_o \tag{7}$$

Where T^T is the transpose of T.

Matrix converter produces the sinusoidal current and voltage waveforms with controllable power factor [63]. The input and output voltages are given in Eq. (8) & (9)

$$V_i(t) = V_{im} \begin{bmatrix} \text{Cos}\ (\omega_i t) \\ \text{Cos}\left(\omega_i t + \frac{2\pi}{3}\right) \\ \text{Cos}\left(\omega_i t + \frac{4\pi}{3}\right) \end{bmatrix} \tag{8}$$

$$V_o(t) = qV_{im} \begin{bmatrix} \text{Cos}\ (\omega_o t) \\ \text{Cos}\left(\omega_o t + \frac{2\pi}{3}\right) \\ \text{Cos}\left(\omega_o t + \frac{4\pi}{3}\right) \end{bmatrix} \tag{9}$$

Where

ω_i, v_i, and v_o are the average input and output voltages and output frequencies.

$$i_o(t) = I_{o\ m} \begin{bmatrix} \text{Cos}\ (\omega_o t + \varphi_o) \\ \text{Cos}\left(\omega_o t + \varphi_o + \frac{2\pi}{3}\right) \\ \text{Cos}\left(\omega_o t + \varphi_o + \frac{4\pi}{3}\right) \end{bmatrix} \tag{10}$$

$$i_i(t) = q\frac{\cos\varphi_o}{\text{Cos}\varphi_o} \begin{bmatrix} \text{Cos}\ (\omega_i t + \varphi_i) \\ \text{Cos}\left(\omega_i t + \varphi_i + \frac{2\pi}{3}\right) \\ \text{Cos}\left(\omega_i t + \varphi_i + \frac{4\pi}{3}\right) \end{bmatrix} \tag{11}$$

Where

φ_i, and φ_o are the input and output displacement angles, and q is the voltage transfer ratio.

3.2. Space vector pulse width modulation

The selection of an appropriate modulation technique is critical for the efficient functioning of converter switches [64]. This study proposes the utilization of the Space Vector Pulse Width Modulation (SVPWM) technique. This technique involves the generation of 27 vectors, categorized into three distinct groups. Group I is characterized by a consistent magnitude of output vectors, which possess the capability to rotate in various directions. Here, each output line is connected to a unique input line, facilitating effective vector control [49]. In Group II, the output vectors undergo changes in magnitude while maintaining a constant direction. These vectors are strategically positioned, separated by intervals of 600 units. This configuration involves connecting one of the output lines to a common input line and the other output line to one of the remaining input lines [51]. Group III features output vectors that lack amplitude, with all output lines converging on a shared input line. The spatial vector representation of the matrix converter is mathematically expressed in Eq. (11), and the corresponding voltage output vectors are illustrated in Fig. 6 [65,64].

$$V_0^{(t)} = \frac{2}{3}\left(V_{ab} + aV_{bc} + a_{ca}^2\right) \tag{12}$$

Where $a = \exp\left(\frac{j2\pi}{3}\right)$

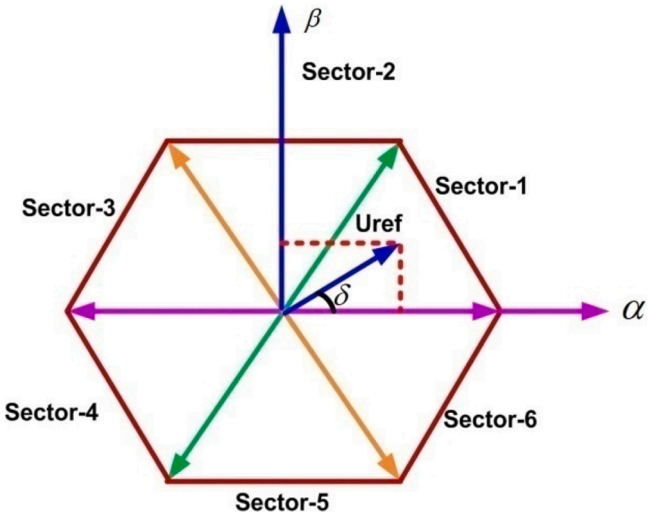

Fig. 6. Output vectors.

The Sliding Mode Controller is non-linear and commonly used to control the non-linearities in system parameters [41]. To ensure the effective functioning of DVR in the presence of faults and load variations, an SMC approach has been suggested and is designed with PI sliding surface and hysteresis control [15].

The direct-quadrature-zero (dqo) transformation, also known as Park Transformation, is a mathematical technique used to simplify controller design and facilitate the analysis of electrical engineering problems involving three-phase systems [66]. This method involves reducing the electrical quantities of the three phases to two-phase electrical quantities [13]. As depicted in Fig. 7, the first step involves feeding the three-phase voltages/currents into the abc/dqo block, which is synchronized with a Phase Lock Loop.

The reference values and actual values are then combined, and the difference is converted into dqo/abc block and then transmitted to the SMC control circuit. The resulting Space Vector Pulse Width Modulation signal is then sent to the matrix converter to control the operation of switches [67]. The error signal will be given to the SMC through a phase lock loop [66]. The direct quadrature zero (dqo) frame reference is also known as Parks Transformation and is used for simplicity in controller design. The three-phase voltages will be converted to two-phase dqo components through the abc/dqo block, and then the difference between actual and reference values will be given to the controller. The controller will supply the difference in parameters to the dqo/abc block, and then this block will convert the dqo parameters into abc. The dqo/abc block will provide information to the PWM block for converter operation [66]. The design of SMC relies on both the selection of a switching function and the formulation of a control law. [43]. The sliding surface makes the system stable, i.e., $S < 0$, where s is a variable, but due to the problem of chattering, the system variables are not reaching zero, i.e., $S > 0$, *as* shown in Fig. 8 [15].

The researchers recommended that the hysteresis band should be utilized to avoid the chattering problem [3]. The differential equations of DVR are given in Eqs. (13 & 14).

$$ki_{cp} = \left(u_p v_{dc} - v_{cp}\right)/L \tag{13}$$

$$kv_{cp} = \left(i_{cp} - i_{sp}\right)/C \tag{14}$$

Where,

$k = d/dt$, i_{cp} is the inductor current, i_{sp} is the supply current, v_{cp} is the voltage compensation, v_{dc} is the chargeable dc supply, u_p is the control input, and L and C are the filter inductance and capacitance. Eq. (15) shows the derivative of compensation voltage [43].

$$x_{1p} = v_{cp} - \dot{v}_{cp},\ x_{2p} = \dot{x}_{1p} = \dot{v}_{cp} - \ddot{v}_{cp} \tag{15}$$

Where,

$\dot{x}_{1p}$ is the derivative of x_{1p} and $\dot{v}_{cp}$ is the derivative of v_{cp}, now take the derivative of Eq. (15).

$$\dot{x}_{1p} = x_{2p} = \dot{v}_{cp} - \ddot{v}_{cp}, \dot{x}_{2p} = \ddot{v}_p - \dddot{v}_p \tag{16}$$

Now submitting the Eq. (12) in $\dot{x}_{2p}$

$$\dot{x}_{2p} = -k\ddot{v}_{cp} + \left(ki_{cp} - ki_{sp}\right)\Big/C \tag{17}$$

Now substitute the Eq. (13) in Eq. (17)

$$\dot{x}_{2p} = -\omega s^2 x_{1p} + \omega s^2 u_p v_{dc} - \omega s^2 \dot{v}_{cp} - k\ddot{v}_{cp} - k\dot{i}_{sp}\Big/C \tag{18}$$

Hence, the behavior of the DVR in terms of

$$x_{1p} \text{ and } x_{2p}\dot{x}_{1p} = x_{2p} \tag{19}$$

$$\dot{x}_{2p} = \omega s^2\left[u_p v_{dc} - x_{1p} + D_p(t)v_{dc}\right] \tag{20}$$

Where $D_p(t)$ is the disturbance

$$D_p(t) = \left(-LKi_{sp} - \dot{v}_{cp} - LC\ddot{V}_{cp}\right) \Big/ v_{dc} \tag{21}$$

From Eq. (21) $D_p(t)$ is the time-varying function. The sliding surface

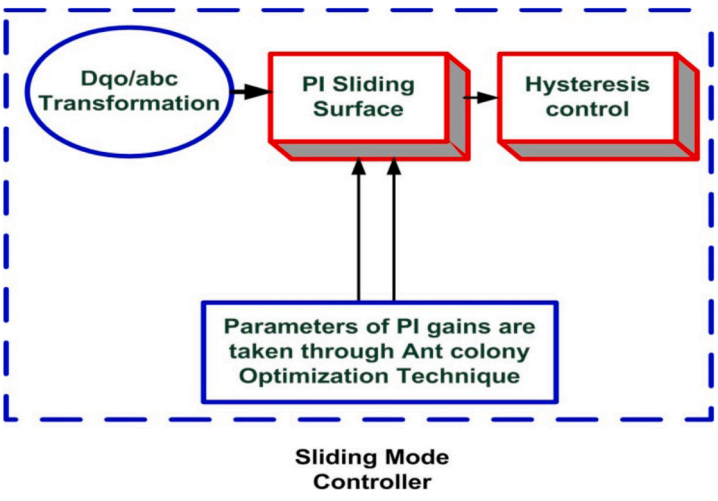

Fig. 7. Proposed sliding mode controller.

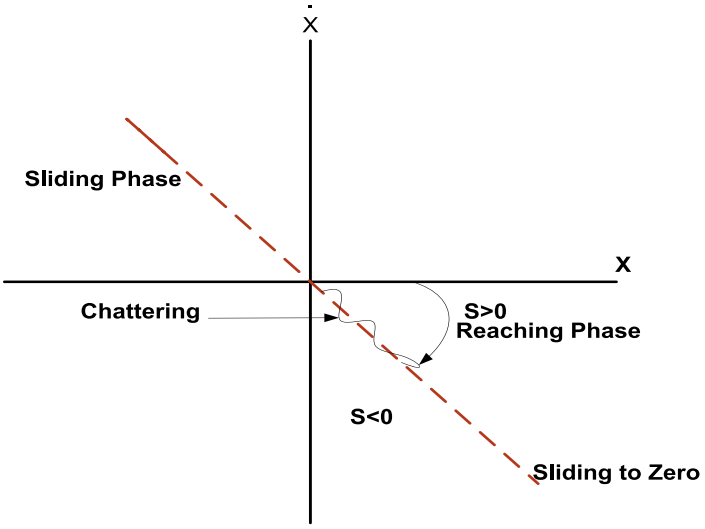

Fig. 8. SMC Phase plot.

is given in Eq. (22).

$$S_p = \lambda x_{1p} + x_{2p} \tag{22}$$

Where λ is the positive sliding surface

3.3. LC filter

The LC filter is presented, which is frequently utilized in converters to mitigate the harmonic distortions caused by converter switching. The proposed filter design aims to effectively reduce these unwanted harmonics and improve the overall performance of the converter. [22]. By referring to Eqs. (23) and (24), it is possible to calculate the output impedance and voltage gain of the LC filter. These equations provide a useful means of analyzing the behavior and performance of the filter, which is essential for optimizing its design and achieving the desired outcomes in converter applications [68].

$$\frac{V_c}{V_s} = \frac{(1 + sRC_2)}{s^3LRC_1C_2 + s^2L(C_1 + C_2) + sRC_2 + 1} \tag{23}$$

Through Eq. (23), we get Eq. (24)

$$H(s) = -R = -\frac{1}{k} = \frac{s^2L(C_1 + C_2 + 1)}{s^3LC_1C_2 + sC_2} \tag{24}$$

The variables R, L, and C represent the resistor, capacitor, and inductor, respectively, in a closed-loop system. The transfer function of the open loop system is represented by H(s), and K is the variable feedback gain.

3.4. Voltage injection transformer

DVR system employs a voltage injection transformer to supply load with the required voltage in case of a shortfall. This device injects the missing voltage into the system as needed, thus ensuring a stable and reliable power supply [48]. In this research paper, 1:1 three single-phase transformers were utilized to compensate the voltage sags individually in each phase [1].

4. ANT colony optimization technique

In this research paper, the ACO technique is proposed to get the optimum value of PI gains [69]. ACO technique in which the activities of the ants are founded on food gathering and selecting the shortest path from the nest to the set objective [70]. Ants can easily communicate with each other through pheromones (chemical signals). Ants can detect pheromones through antennas and leave the pheromones in the soil for follow-up with the other ants. [71,72]. The flow chart of the ACO technique is shown in Fig. 9 [69]. The node selection is calculated through heuristic, and pheromone factors are given in Eq. (25) [70]. The heuristic factor is denoted by n_{ij} and the pheromone factor is denoted by τ_{ij}.

$$[\tau_{ij}]\alpha[n_{ij}]\beta \tag{25}$$

Where α and β are constants that calculate the kin effect of the pheromone values and the heuristic values, the probability of distribution is calculated through Eq. (26) [70].

$$\rho_{ij} = \frac{[\tau_{ij}]\alpha[n_{ij}]\beta}{\sum_{h\in S}[\tau_{ih}]\alpha[n_{ih}]\beta} \tag{26}$$

In the ACO technique, the cost function is used for controller design [73]. The scientific community suggested the three cost functions; the utilization will depend on the controller design [74]. In the first cost

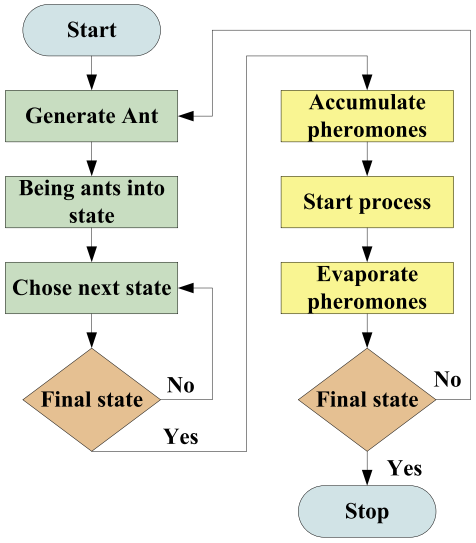

Fig. 9. Flow chart of ACO technique.

function, the value of the integrated square will be reduced, as given in Eq. (27) [70].

$$f_1 = \int_0^{\infty} (e^t dt)2 \tag{27}$$

The second cost function is determined by the cumulative values of the rise time, maximum overshoot, steady-state error, and settling time. [75] and given in Eq. (28).

$$f_2 = \frac{1}{\left[C_1\ (t_r - t_{rd}) + C_2\ \left(M_p - M_{pd}\ \right) + C_3\ (t_s - t_{ds}) + C_4(e_{ss} - e_{ssd})\right]} \tag{28}$$

The third cost function, as expressed in Eq. (29), indicates that the choice of α and β values is crucial in determining the optimal design of a controller. In other words, the selection of these values plays a significant role in the controller's performance and effectiveness. Therefore, it is important to carefully consider and evaluate different options for α and β to ensure the controller operates as intended and meets the desired objectives. Ultimately, the appropriate selection of these parameters can lead to improved system stability, accuracy, and responsiveness [76].

$$f_3 = \frac{1}{(1 - e^{-\beta})(M_p + e_{ss}) + e^{-\beta}(t_s - t_r)} \tag{29}$$

The cost VS iteration curve is shown in Fig. 10. The cost is decreasing with iterations [70].

The parameters in Table 2 are utilized in the ACO MATLAB program [70], and the best values of PI gains obtained after the completion of 50 iterations are given in Table 3.

5. Methodology

The distribution system with the proposed DVR is shown in Fig. 11 [1].

The performance of the SMC with matrix converter-based DVR was analyzed using MATLAB simulation software under single phase to ground fault and load variations. The parameters in Table 4 are utilized to obtain the simulation results [5].

The distribution network in question comprises an 11 kV feeder and a step-down distribution transformer rated at 11kV/400Volts with a capacity of 50 kVA, serving a three-phase RL load. The DVR framework integrates a Phase-Locked Loop (PLL) with dq_0 transformation, which facilitates error detection in parameters and simplifies controller design. A Sliding Mode Controller (SMC) equipped with hysteresis control and a

Table 2
ACO Parameters.

S.No	Parameter	Value
1	Alpha (α)	0.8
2	Beta (β)	0.2
3	Rho	0.7
4	Nodes	1000
5	Upper bound	[10 10 10 10]
6	Lower bound	[−10 −10 −10 −10]
7	No. of Ants	50
8	No. of Iterations	50

Table 3
Parameters of PI gains.

S. No	Parameters of PI Gains	
1	Kp=−6.87688	Kp=−2.517
2	Ki=0.850851	Ki=2.219

PI sliding surface is employed to manage the DVR dynamics. For the accurate operation of the matrix-converter switches, a three-phase matrix converter utilizing Space Vector Pulse Width Modulation (SVPWM) is employed alongside an LC filter to mitigate harmonics. To address voltage compensation needs, three single-phase voltage injection transformers with a 1:1 ratio are used to inject the required voltage into the load as needed. Fault conditions were simulated with a single phase to ground fault over 60 milliseconds, featuring 0.01 ohm fault resistance and 0.001 ohm ground resistance. Additionally, the DVR's performance was evaluated under varied load conditions (30kW, 70 kW, and 120 kW) without faults using MATLAB simulation software.

6. Simulation results and discussion

6.1. Single line to ground fault condition

When a fault is applied to one phase of three phase system then we have seen that the supply voltage is reduced to 100 Volts. This condition is not acceptable for sensitive loads, so timely compensation is essential. The system voltage, load voltage, load current, and voltage injection through DVR are shown in Figs. 12(a), 12(b), 12(c), and 12(d). In Figures (b) and (c), it have been seen that the DVR compensate the missing voltage and maintain the load current without any overshoot. The selected controller is appropriate for DVR under this fault condition and settled at the time of 0.02 s.THD of the proposed controller was

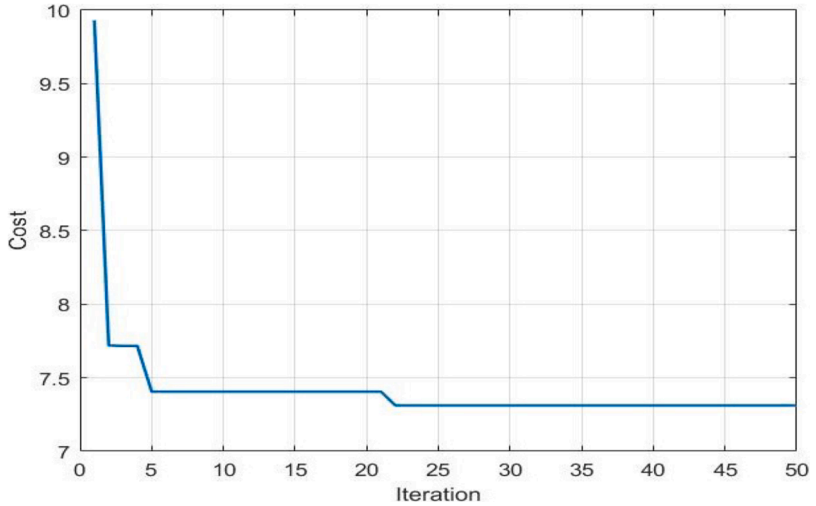

Fig. 10. Cost VS Iteration curve.

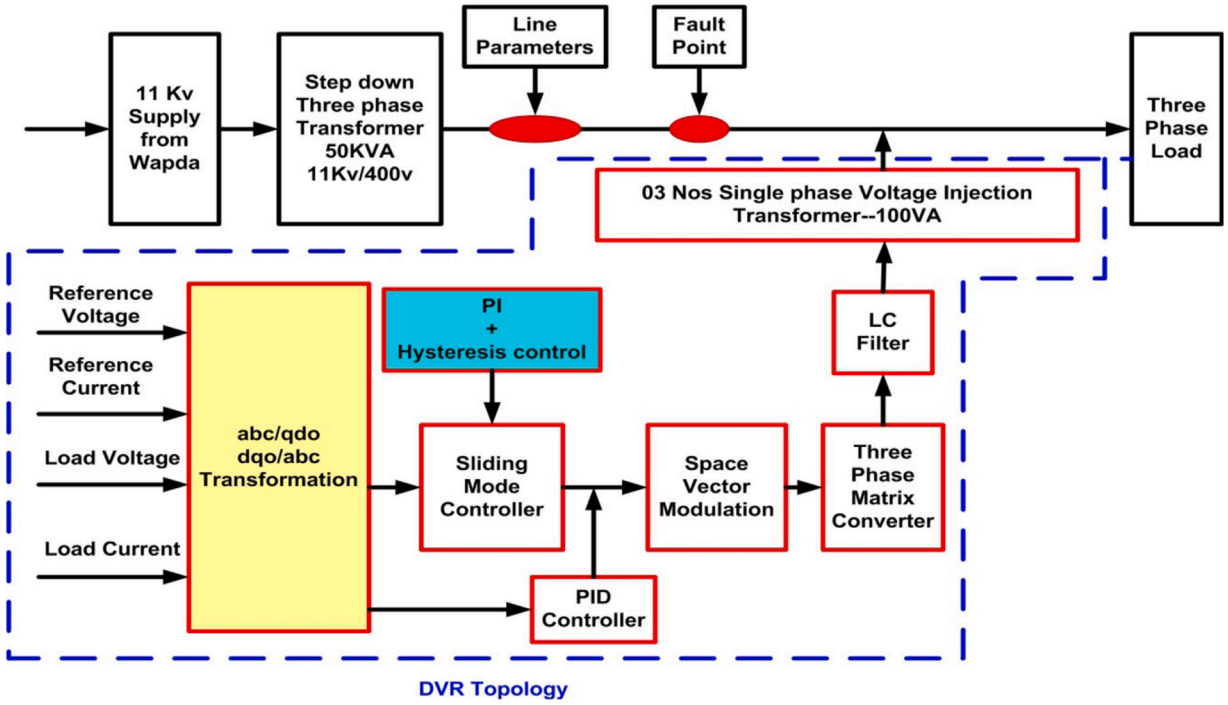

Fig. 11. Proposed power system with DVR topology.

Table 4
Parameters of proposed power system with DVR.

S. No	Parameter	Value
1	Grid voltage	11k V
2	Distribution transformer (11KV/400 Volts)	100 kVA
3	Supply voltage to load	400Volts
4	Line parameters	R = 0.001ohm, L = 16.58 e-6 H
5	Three-phase load with single-phase fault	5k W
6	LC Filter	5.8mH, 2e-6 farad
7	Three single-phase voltage injection transformers	1:1
8	Fault time	60 milli-seconds
9	Fault Resistance	0.01 ohms
10	Ground resistance	0.001 ohms
11	System frequency	50 Hz
12	Switching frequency	6 kg-Hz
13	Three-phase loads without fault condition	30k W, 70k W, and 120 kW

acceptable as per IEEE standards 519–1992 [77] i.e., 2.56 %, so the SMC controller is appropriate for DVR under fault and load variations. Simulation results of SMC with DVR are given in Table 5.

6.2. *Performance of sliding mode controller at 30 kW load*

To ascertain the robustness of the SMC, its performance was rigorously assessed under various load conditions. Specifically, when subjected to a 30 kW load, the load voltage experienced a 12 % reduction. In response, the Dynamic Voltage Restorer (DVR) effectively sustained both the load voltage and current. The operational parameters, encompassing the system voltage, load voltage, load current, and the voltage compensation executed by the DVR, are comprehensively depicted in Figs. 13(a), 13(b), 13(c), and 13(d).

6.3. *Performance of sliding mode controller at 70 kW load*

Under a 70 kW load condition, where the load voltage diminished by 27 %, the Dynamic Voltage Restorer (DVR) successfully upheld the voltage and current on the load side. Illustrations of the system voltage, load voltage, load current, and the voltage adjustment facilitated by the DVR are methodically presented in Figs. 14(a), 14(b), and 14(c).

6.4. *Performance of sliding mode controller at 120 kW load*

Upon experiencing a load of 120 kW, which resulted in a 39 % reduction in load voltage, the Dynamic Voltage Restorer (DVR) adeptly

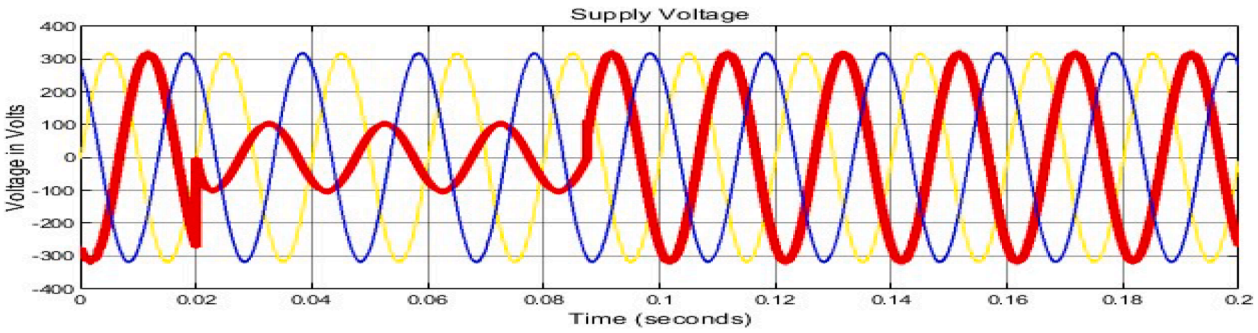

Fig. 12a. System voltage under single-phase fault.

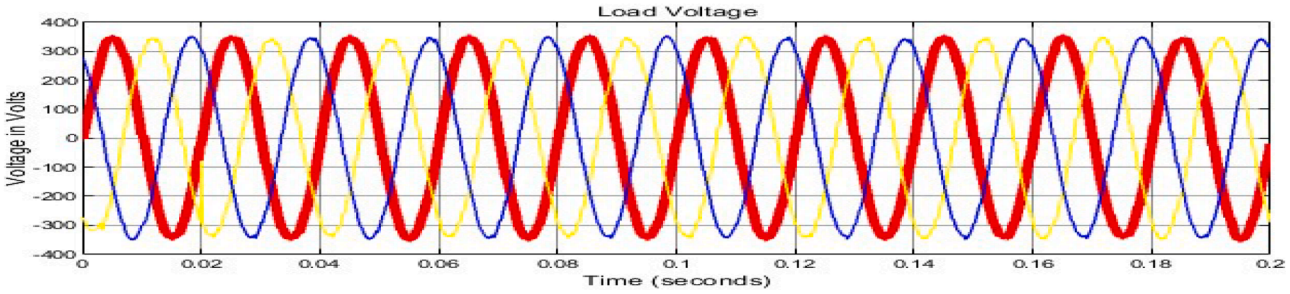

Fig. 12b. Load voltage with SMC under single-phase fault.

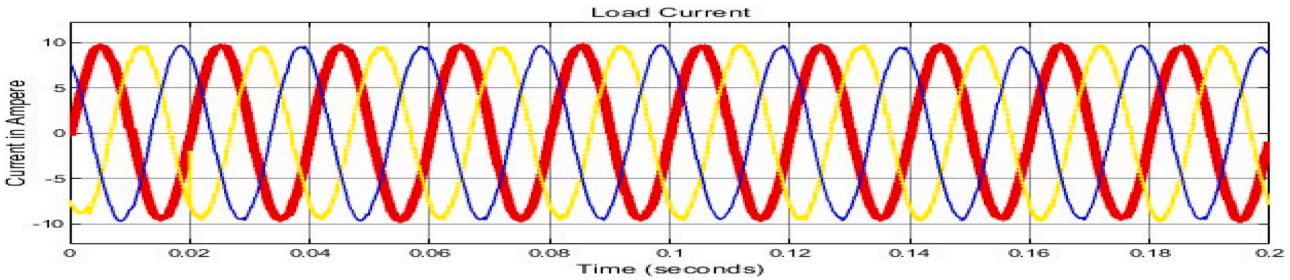

Fig. 12c. Load current with SMC under single-phase fault.

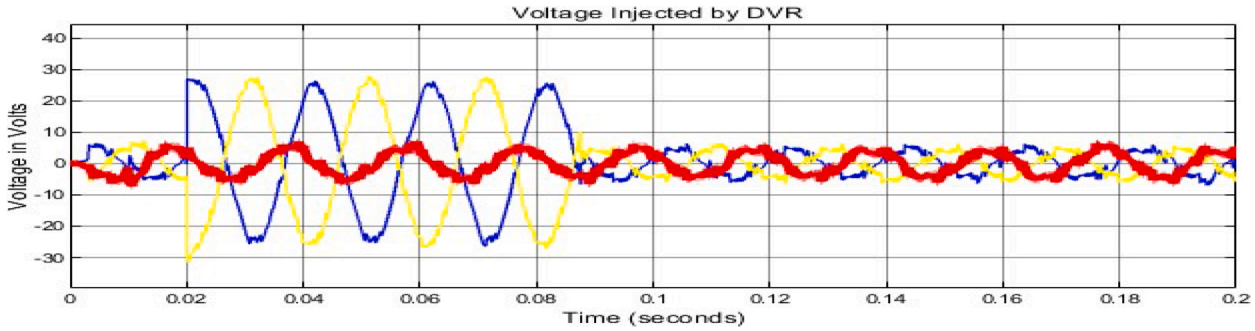

Fig. 12d. Voltage injection through DVR with SMC under single-phase fault.

Table 5
Simulation results of proposed DVR with SMC Controller.

Parameter	Single phase fault	30 kW Load	70 kW Load	120 kW Load
Voltage Sag	227 Volts	40 Volts	88 Volts	127 Volts
Voltage overshoot	No	No	No	No
Current overshoot	No	No	No	No
Settling Time	From where fault time was started, i.e., 0.02 s	From where voltage sag was started	From where voltage sag was started	From where voltage sag was started
THD%	2.56 %			

maintained the voltage and current levels on the load side. The load voltage, load current, and voltage compensation executed by the DVR are effectively demonstrated in Figs. 15(a), 15(b), and 15(c). The THD under single line fault is evaluated by FFT method and is shown in Fig. 16, it has seen that the 2.56 % is within the standards [77], so the selected controller is fit under load variations. Simulation results of SMC with DVR are given in Table 5.

6.5. Total harmonic distortion percentage with smc controller (THD %)

The THD% of the proposed DVR with SMC controller was analyzed through FFT and is shown in Fig. 16. The THD% of the proposed controller was acceptable as per IEEE standards 519–1992 [77], i.e., 2.56 %, so the SMC controller is appropriate for DVR under fault and load variations. Simulation results of SMC with DVR are given in Table 5.

6.6. Performance of pid controller under single line to ground fault condition

In this fault condition the yellow phase experience a load voltage drop of up to 70 percent. The voltage system, effect on load voltage, and

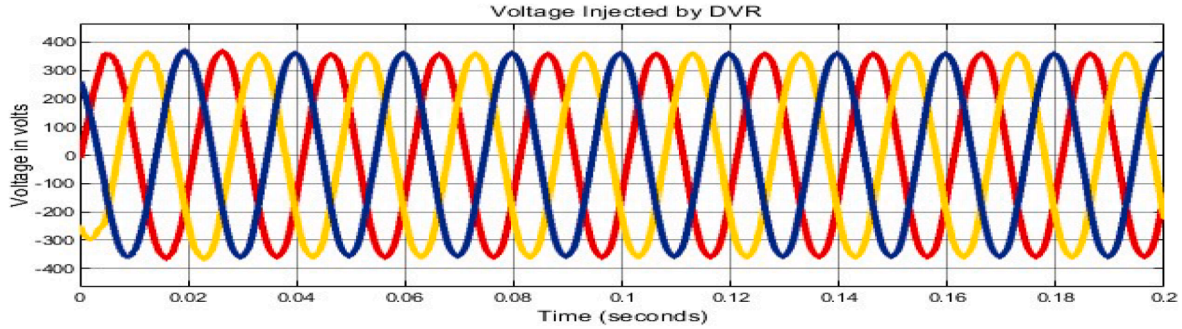

Fig. 13a. Normal system voltage.

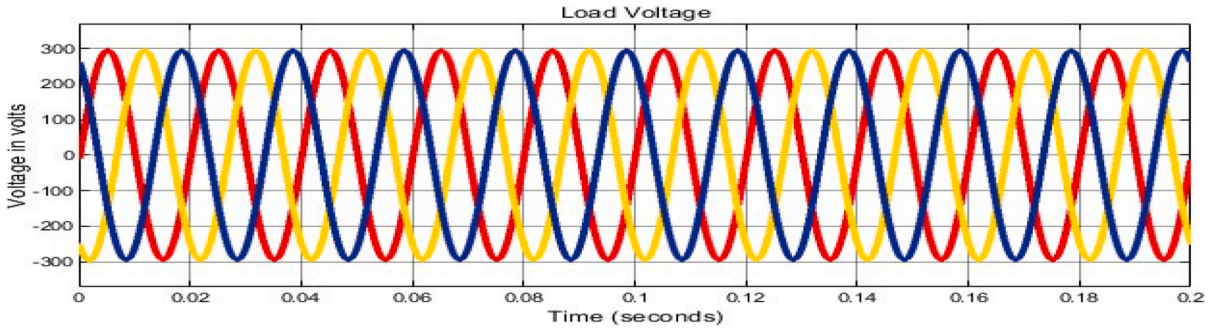

Fig. 13b. 12 % Decreases in load voltage at 30 kW Load.

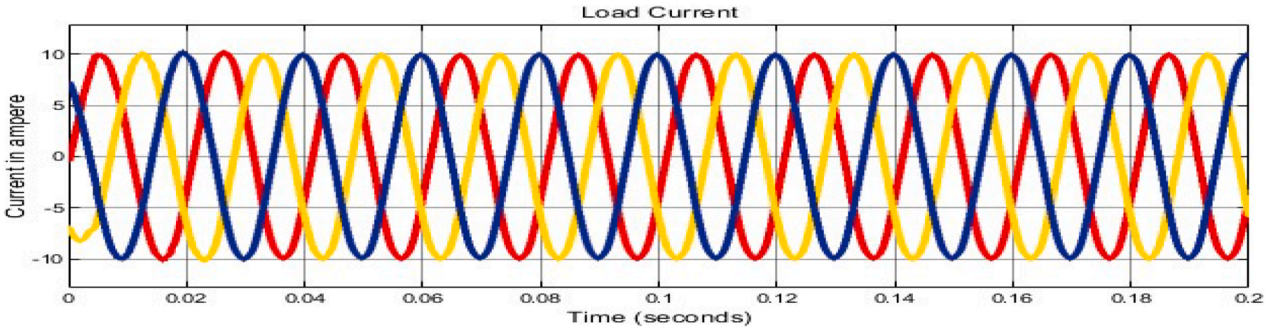

Fig. 13c. Load current maintained by DVR during 12 % decrease in V_L at 30 kW Load.

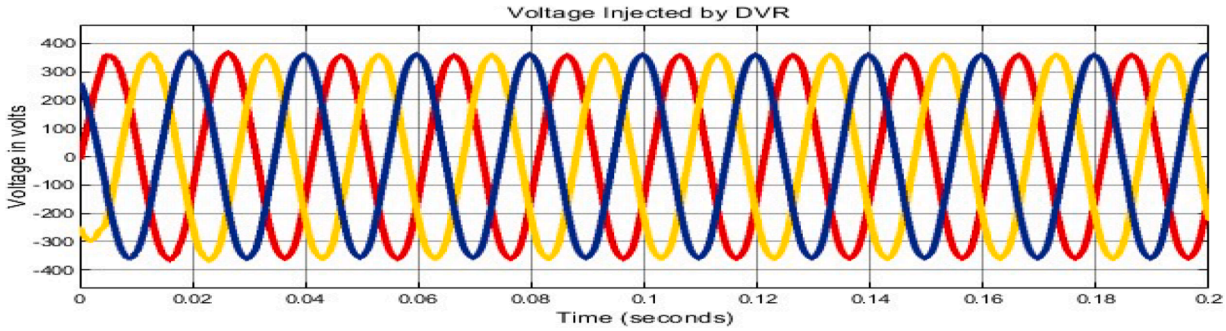

Fig. 13d. Voltage injected by DVR during 12 % decreased in V_L at 30 kW Load.

voltage injection through DVR is shown in Figs. 17(a), 17(b), and 17(c) respectively. As is seen, the output load voltage is not appropriately regulated through the DVR and is higher than normal value because of using of linear PID controller and settled at the time of 0.04 s which may be damaging on more sensitive loads. The THD of DVR with PID controller is also analyzed under single phase fault condition, so it has been seen that the THD is 12.41 % of fundamental frequency and also not acceptable as IEEE standards is shown in Fig. 18.

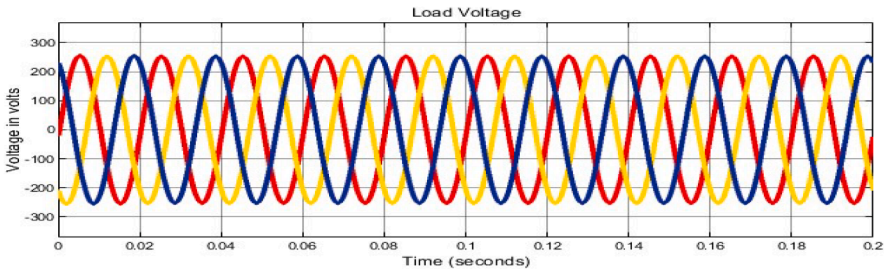

Fig. 14a. 27 % Decrease in load voltage at 70 kW.

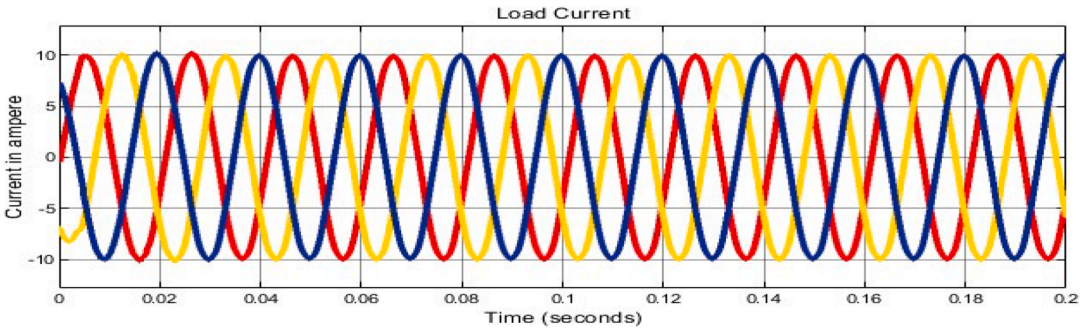

Fig. 14b. Load current maintained by DVR during 27 % decrease in V_L at 70 kW Load.

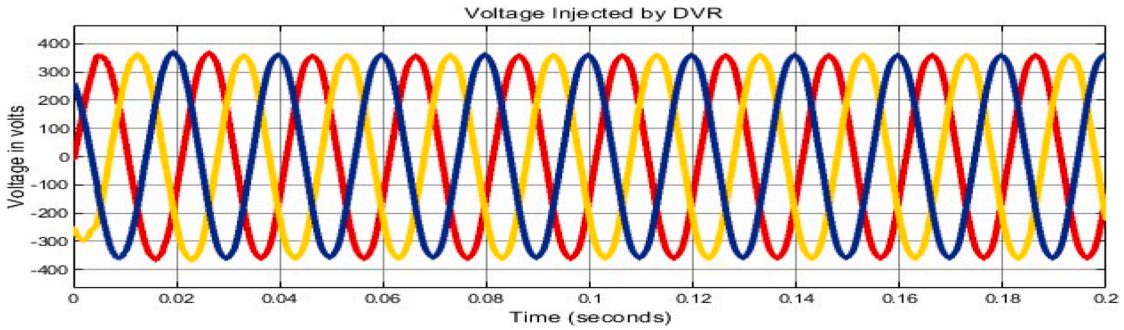

Fig. 14c. Voltage injected by DVR during a 27 % decrease in Load Voltage at 70 kW Load.

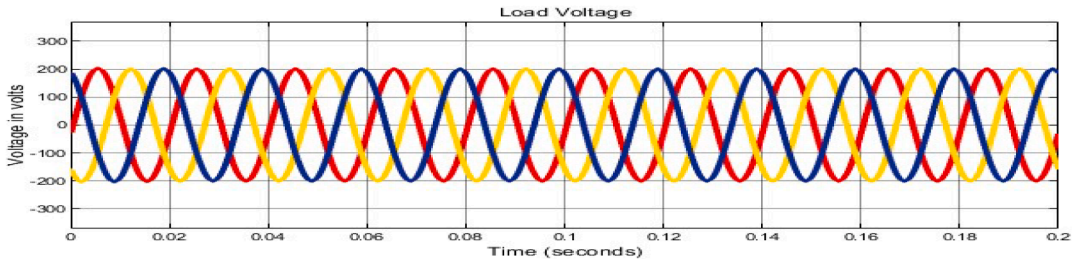

Fig. 15a. 39 % decrease in load voltage at 120 kW.

6.7. Discussion

The effectiveness of a matrix converter-based DVR employing a SMC strategy was assessed using MATLAB simulation software. The evaluation scrutinized the system's responsiveness under various load scenarios and in the event of a single-phase fault. The simulation findings underscore the matrix converter's proficiency in executing direct AC-AC voltage conversion, thereby circumventing the necessity for auxiliary conversions, energy storage units, and charging mechanisms. This inherent attribute of the matrix converter design potentially contributes to the diminution of both installation and operational expenditures associated with DVR systems. Additionally, the absence of energy storage components not only trims down the system's footprint but also simplifies the integration into areas where space is at a premium. Upon the imposition of voltage sag to 227 Volts during a single-phase fault, the system demonstrated the ability to sustain the load voltage and current satisfactorily. Further scrutiny under varying load conditions specifically at 30 kW, 70 kW, and 120 kW was conducted to verify the SMC

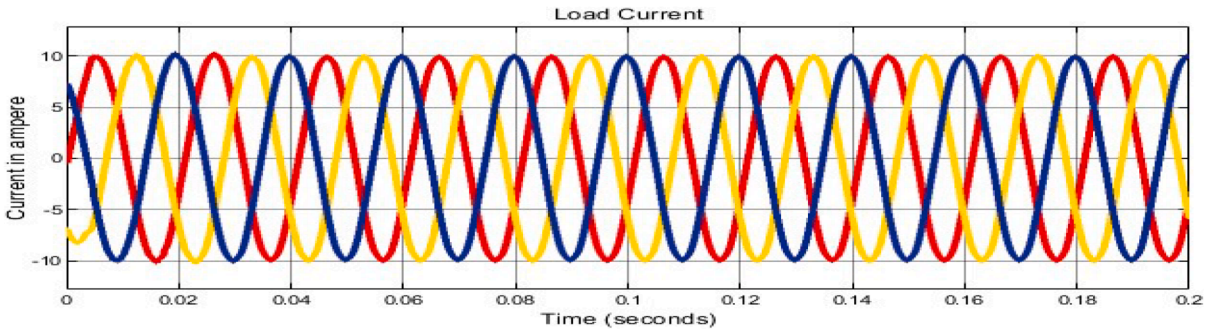

Fig. 15b. Load current maintained by DVR during a 39 % decrease in V_L at 120 kW Load.

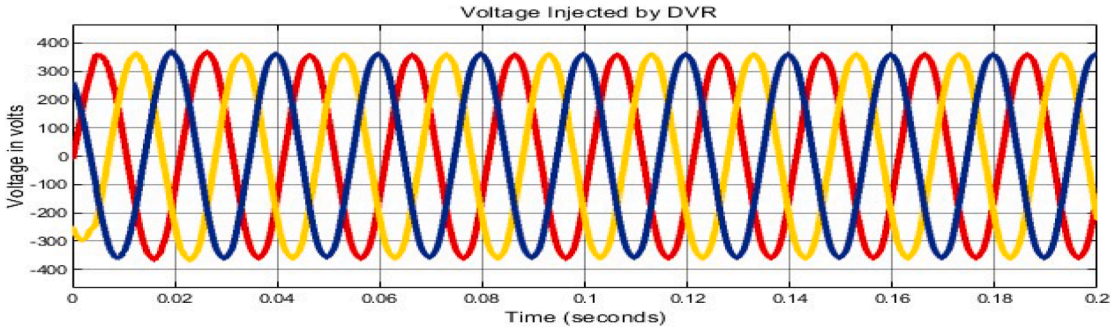

Fig. 15c. Voltage injected by DVR during 39 % decreased in V_L at 120 kW Load.

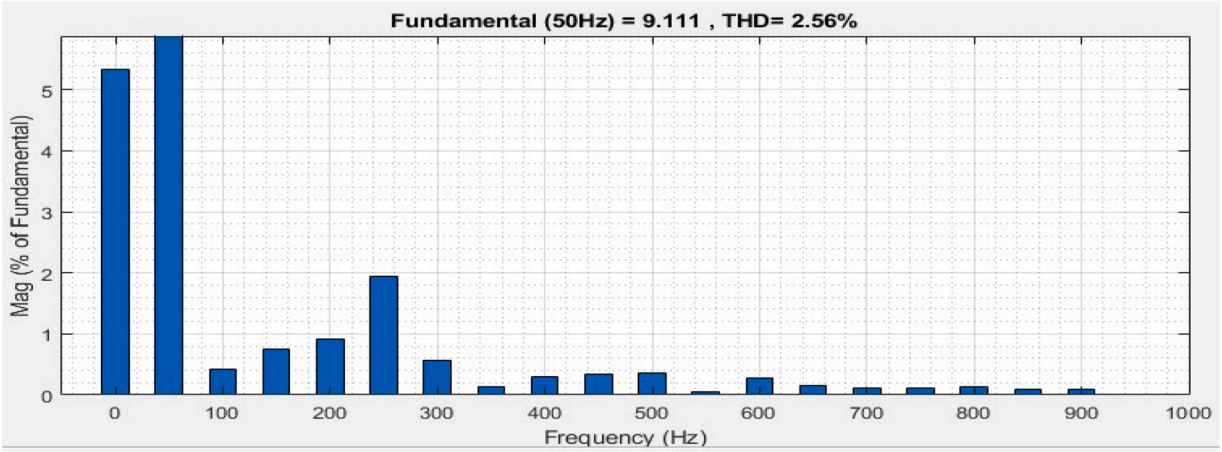

Fig. 16. THD with SMC.

controller's robustness. The SMC showcased commendable performance across these diverse load settings. The THD% of the proposed controller was examined using the Fast Fourier Transform (FFT), revealing a THD % less than 5 % of the fundamental frequency, which indicates a favorable control approach for the DVR topology during fault incidents and across a spectrum of load conditions. Analyzing the formula derived for the DVR topology, it was identified that the proposed controller is a superior and improved control approach for the topology. This work provides a real practical solution on Matrix Converter based DVR control for the engineers and researchers in order to implement it in actual power system problem. The emphasis on effectiveness adds much more value and importance to the topic within the respective discipline. The PID controller is not appropriate for DVR under fault condition and also THD is 12.41 % of fundamental frequency, which is not acceptable as per IEEE standards and settled at the time of 0.04 s. The comparison between MC and VSI is given in Table 6.

7. Conclusion

The application of a Matrix Converter-based Dynamic Voltage Restorer (DVR) integrated with a Sliding Mode Control (SMC) and optimized via the Ant Colony Optimization (ACO) technique manifests as a highly proficient solution for the rectification of voltage sags. This avant-garde technology brings a plethora of enhancements and benefits to the domain of power quality improvement. Notably, the Matrix Converter-based DVR signifies a substantial leap forward from traditional voltage source converters, delivering a solution that is both compact and efficient. Its adeptness at direct AC-to-AC power conversion obviates the need for intermediary energy storage mechanisms, thereby diminishing the system's complexity, as well as its cost and

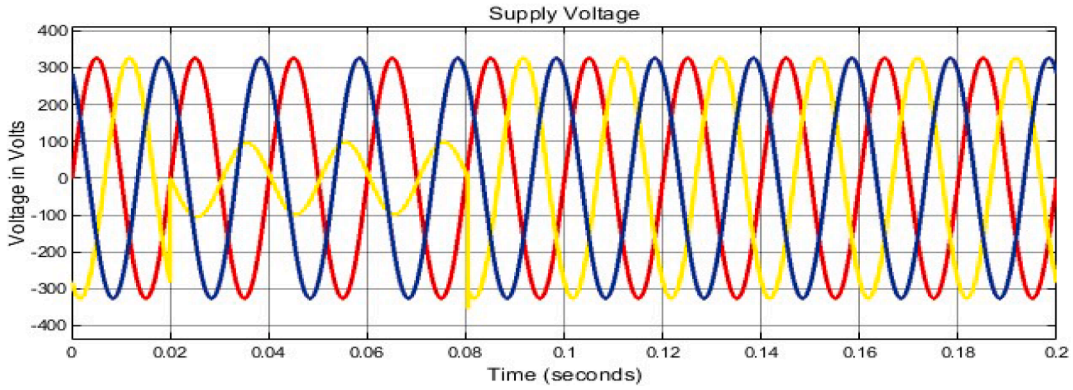

Fig. 17a. Sag voltage with PID under Single-phase Fault.

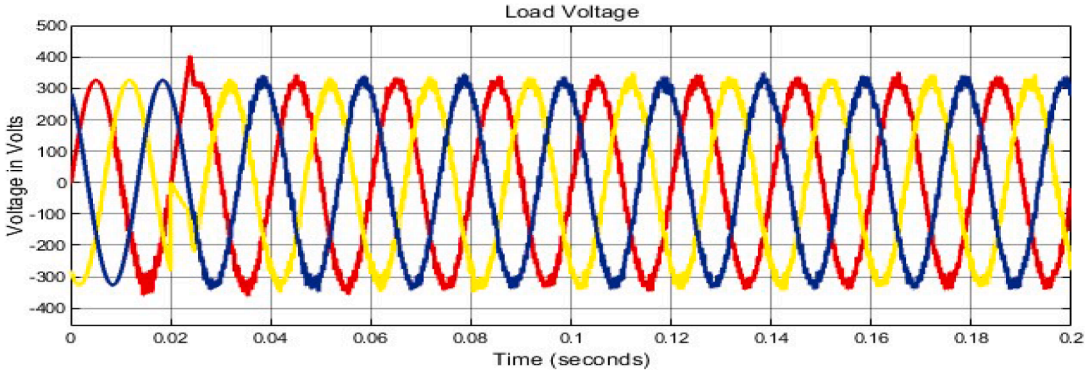

Fig. 17b. Load Voltage with PID under Single-phase Fault.

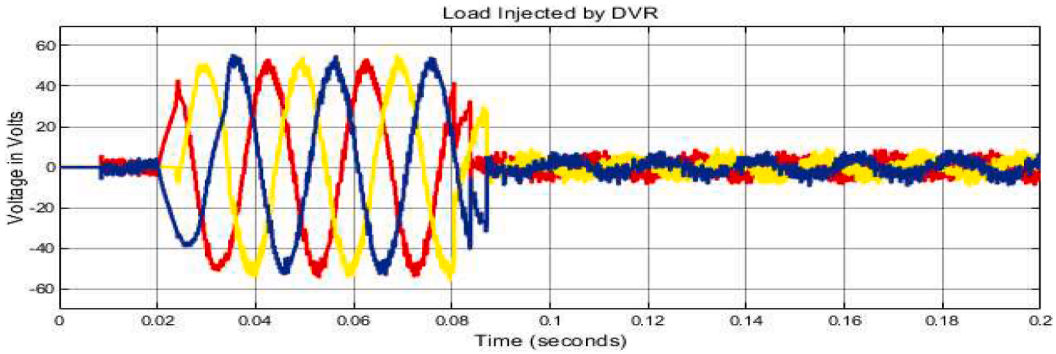

Fig. 17c. Voltage Injected by DVR with PID Controller.

physical footprint. The assimilation of SMC into the DVR's operation elevates its performance, ensuring stable and accurate voltage regulation. The SMC, particularly when its parameters are optimized using the ACO technique, excels in disturbance rejection and maintains robustness amidst parameter uncertainties and varying load conditions. This adaptability is crucial for the DVR's rapid and effective response to voltage sags, ensuring the reliability of the power supply to sensitive loads. Another salient feature of this integrated system is its support for bidirectional power flow, facilitating energy exchange between the grid and the load, which enhances power transfer efficiency and enables potential energy regeneration, aligning with sustainable operational practices. In addition, the Matrix Converter-based DVR, with its SMC-ACO framework, extends superior fault ride-through capabilities, reinforcing the stability and dependability of the power system during voltage disturbances. The swift response and meticulous voltage compensation afforded by this system are instrumental in reducing production lapses and averting equipment damage, thereby enhancing the overall performance of the system and reducing operational interruptions. In conclusion, the amalgamation of a Matrix Converter-based DVR with an SMC control strategy, fine-tuned by the ACO technique, constitutes a highly effective and efficient remedy for voltage sag challenges. This innovative technology proffers numerous advantages, including compact design, bidirectional power flow, enhanced fault tolerance, and steadfast voltage regulation. Its adoption could significantly mitigate the adverse impacts of voltage sags, ameliorate power quality, and assure the uninterrupted operation of critical loads. Future research endeavors should focus on evaluating the scalability of this approach for more extensive grid systems, its integration with renewable energy sources, and its economic and environmental sustainability over prolonged periods. Furthermore, empirical testing under various

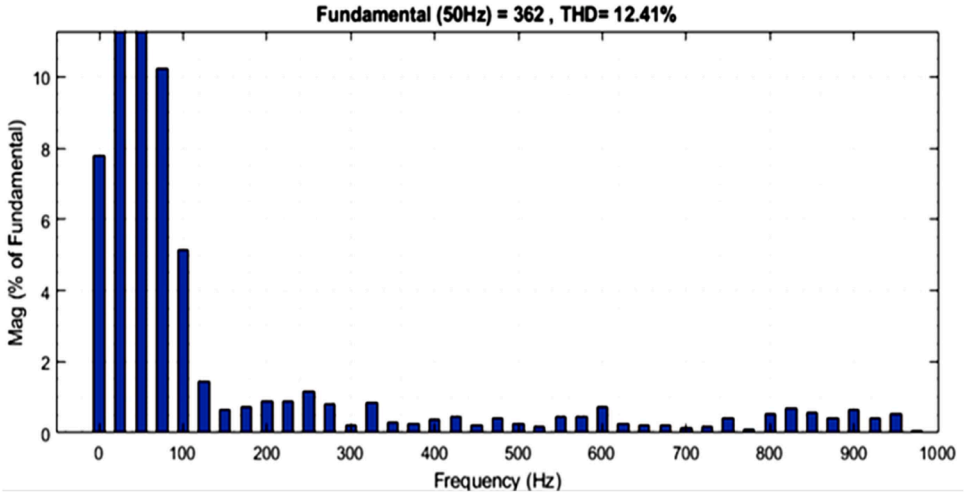

Fig. 18. THD with PID Controller.

Table 6
Comparison between MC and VSI at 5KW load [11].

Component/Equipment	Matrix Converter	Voltage Source Inverter
IGBT switches	18 Nos	12 Nos
Clamp diodes	12 Nos	0
Capacitors	3 Nos	3 Nos
Inductors	3 Nos	6 Nos
Gate units	18 Nos	12 Nos
Voltage measurements	2 Nos	3 Nos
Current measurements	4 Nos	6 Nos
Installed switch power	756/105 (KVA/%)	720/100 (KVA/%)
DC link capacitor	Not Required	750 μF. The cost is six times higher than clamp diodes.
Current ripple factor	Low	15 % higher than the peak fundamental current
Losses at higher switching frequencies	Low	High
Energy storage unit (Battery)	Not Required	Required which include high installation and maintenance cost
Installation and maintenance cost	Low	High

real-world grid scenarios would provide invaluable insights, enabling further refinement and customization of the system for widespread application.

CRediT authorship contribution statement

Abdul Hameed Soomro: Writing – original draft, Validation, Software, Methodology, Investigation, Conceptualization. **Abdul Sattar Larik:** Writing – original draft, Validation, Supervision, Software, Methodology, Investigation. **Mukhtiar Ahmed Mahar:** Writing – original draft, Validation, Supervision, Software, Methodology, Formal analysis, Conceptualization. **Anwer Ali Sahito:** Writing – original draft, Visualization, Formal analysis, Data curation. **Mohsin Ali Koondhar:** Writing – original draft, Validation, Software, Methodology, Investigation, Conceptualization. **Yun-Su Kim:** Writing – review & editing, Visualization, Resources, Methodology, Data curation. **Zuhair Muhammed Alaas:** Writing – review & editing, Visualization, Formal analysis, Data curation. **Ezzeddine Touti:** Writing – review & editing, Validation, Methodology, Investigation, Funding acquisition. **M.M.R. Ahmed:** Writing – review & editing, Visualization, Formal analysis, Data curation.

Declaration of competing interest

The authors declare that they have no known competing financial interests or personal relationships that could have appeared to influence the work reported in this paper.

Acknowledgments

This work was supported by GIST Research Project grant funded by the GIST in 2024. Also the authors extend their appreciation to the Deanship of Scientific Research at Northern Border University, Arar, KSA for funding this research work through the project number "NBU-FFR-2025-2448-20".

Data availability

Data will be made available on request.

References

[1] A.H. Soomro, et al., Dynamic Voltage Restorer—A comprehensive review, Energy Rep. 7 (2021) 6786–6805.
[2] S. Srivastava, S. Singh, A. Yadav, Analysis of Voltage Sag and THD Using Dynamic Voltage Restorer, in: 2022 S International Conference on Artificial Intelligence and Smart Energy (ICAIS), IEEE, 2022.
[3] S.T. Zahra, et al., Simulation-based analysis of dynamic voltage restorer with sliding mode controller at optimal voltage for power quality enhancement in distribution system, Electr. Eng. & Electromechanics (1) (2022) 64–69.
[4] R. Adware, V. Chandrakar, Comprehensive Analysis of STATCOM with SVC for Power Quality Improvement in Multi Machine Power System, in: 2022 2nd International Conference on Power Electronics & IoT Applications in Renewable Energy and its Control (PARC), IEEE, 2022.
[5] A.H. Soomro, et al., Simulation-based Analysis of a Dynamic Voltage Restorer under Different Voltage Sags with the Utilization of a PI Controller, Eng. Technol. Appl. Sci. Res. 10 (4) (2020) 5889–5895.
[6] B. Pattanaik, et al., Energy storage system with dynamic voltage restorer integrated for wind energy system, in: Journal of Physics: Conference Series, IOP Publishing, 2021.
[7] K. Jeyaraj, D. Durairaj, A.I.S. Velusamy, Development and performance analysis of PSO-optimized sliding mode controller–based dynamic voltage restorer for power quality enhancement, Int. Trans. Electr. Energy Syst. 30 (3) (2020) e12243.
[8] A.H. Soomro, et al., Simulation-Based Comparison of PID with Sliding Mode Controller for Matrix-Converter-Based Dynamic Voltage Restorer under Variation of System Parameters to Alleviate the Voltage Sag in Distribution System, Sustainability. 14 (21) (2022) 14661.
[9] K.B. Tawfiq, M.N. Ibrahim, P. Sergeant, An enhanced fault-tolerant control of a five-phase synchronous reluctance motor fed from a three-to-five-phase matrix converter, IEEe J. Emerg. Sel. Top. Power. Electron. 10 (4) (2022) 4182–4194.
[10] J. Zhang, et al., A review of control strategies for flywheel energy storage system and a case study with matrix converter, Energy Rep. 8 (2022) 3948–3963.
[11] S. Bernet, S. Ponnaluri, R. Teichmann, Design and loss comparison of matrix converters, and voltage-source converters for modern AC drives, IEEE Trans. Ind. Electron. 49 (2) (2002) 304–314.

[12] A. Dendouga, A comparative study between the PI and SM controllers used by nonlinear control of induction motor fed by SVM matrix converter, IETe J. Res. 68 (4) (2022) 3019–3029.
[13] A.H. Soomro, et al., Mathematical Modeling and Simulation of AC-AC Three Phase Matrix Converter with LC Filter driving Static Resistive Load, Quaid-E-Awam Univ. Res. J. Eng., Sci. & Technol., Nawabshah 20 (02) (2022) 107–113.
[14] R. Zhang, et al., An Asymmetric Hybrid Phase-Leg Modular Multilevel Converter with Small Volume, Low Cost, and DC Fault-Blocking Capability, IEEe Trans. Power. Electron. (2024).
[15] N. Kassarwani, J. Ohri, A. Singh, Performance analysis of dynamic voltage restorer using improved PSO technique, Int. J. Electron. 106 (2) (2019) 212–236.
[16] Z.Y. Nie, et al., A unifying Ziegler–Nichols tuning method based on active disturbance rejection, Int. J. Robust. Nonlinear. Control 32 (18) (2022) 9525–9541.
[17] K. Deželak, et al., Proportional-integral controllers performance of a grid-connected solar PV system with particle swarm optimization and Ziegler–Nichols tuning method, Energies. (Basel) 14 (9) (2021) 2516.
[18] Q. Han, et al., A triboelectric rolling ball bearing with self-powering and self-sensing capabilities, Nano Energy 67 (2020) 104277.
[19] X. Ju, et al., Quantized predefined-time control for heavy-lift launch vehicles under actuator faults and rate gyro malfunctions, ISA Trans. 138 (2023) 133–150.
[20] J. Chen, et al., Enhanced Modular Multilevel Converter with Multiple MVac Ports Based on Active Fundamental-Frequency Circulating Current Injection to Realize Full-Range Operation, IEEe Trans. Power. Electron. (2024).
[21] S. Fidanova, S. Fidanova, Ant colony optimization, Ant Colony Optimization and Appl. (2021) 3–8.
[22] A.M. Saeed, et al., Power conditioning using dynamic voltage restorers under different voltage sag types, J. Adv. Res. 7 (1) (2016) 95–103.
[23] C. Curry, Lithium-ion battery costs and market, Bloomberg New Energy Finance 5 (4–6) (2017) 43.
[24] C. Vaalma, et al., A cost and resource analysis of sodium-ion batteries, Nat. Rev. Mater. 3 (4) (2018) 1–11.
[25] J. Tan, et al., Event-triggered sliding mode control for spacecraft reorientation with multiple attitude constraints, IEEE Trans. Aerosp. Electron. Syst. 59 (5) (2023) 6031–6043.
[26] K. Ma, J. Yang, P. Liu, Relaying-assisted communications for demand response in smart grid: cost modeling, game strategies, and algorithms, IEEE J. Sel. Areas Commun. 38 (1) (2019) 48–60.
[27] J. Zhang, et al., Series–shunt multiport soft normally open points, IEEE Trans. Ind. Electron. 70 (11) (2022) 10811–10821.
[28] Y. Li, et al., Load profile inpainting for missing load data restoration and baseline estimation, IEEe Trans. Smart. Grid. (2023).
[29] Y.-H. Lan, J.-Y. Zhao, Improving Track Performance by Combining Padé-Approximation-Based Preview Repetitive Control and Equivalent-Input-Disturbance, J. Electrical Eng. Technol. (2024) 1–14.
[30] J. Hang, et al., Interturn Short-Circuit Fault Diagnosis and Fault-Tolerant Control of DTP-PMSM Based on Subspace Current Residuals, IEEe Trans. Power. Electron. (2024).
[31] S. Li, et al., A reduced current ripple overmodulation strategy for indirect matrix converter, IEEE Trans. Ind. Electron. (2024).
[32] N. Li, et al., An Improved Modulation Strategy for Single-Phase Three-Level Neutral-Point-Clamped Converter in Critical Conduction Mode, J. Mod. Power Syst. Clean Energy (2024).
[33] M. Shirkhani, et al., A review on microgrid decentralized energy/voltage control structures and methods, Energy Rep. 10 (2023) 368–380.
[34] H. Wang, et al., A thermal network model for multichip power modules enabling to characterize the thermal coupling effects, IEEe Trans. Power. Electron. (2024).
[35] L. Fang, D. Li, R. Qu, Torque improvement of vernier permanent magnet machine with larger rotor pole pairs than stator teeth number, IEEE Trans. Ind. Electron. 70 (12) (2023) 12648–12659.
[36] Q. Rong, et al., Virtual external perturbance-based Impedance measurement of grid-connected converter, IEEE Trans. Ind. Electron. (2024).
[37] Q. Rong, et al., Asymmetric sampling disturbance-based universal impedance measurement method for converters, IEEe Trans. Power. Electron. (2024).
[38] F. Song, et al., Motion Control of Wafer Scanners in Lithography Systems: from Setpoint Generation to Multi-Stage Coordination, IEEe Trans. Instrum. Meas. (2024).
[39] S. Gao, et al., An efficient half-bridge mmc model for emtp-type simulation based on hybrid numerical integration, IEEE Trans. Power Syst. 39 (1) (2023) 1162–1177.
[40] S. DaneshvarDehnavi, et al., Dynamic Voltage Restorer (DVR) with a novel robust control strategy, ISA Trans. 121 (2022) 316–326.
[41] R. Nasrollahi, et al., Sliding mode control of a dynamic voltage restorer based on PWM AC chopper in three-phase three-wire systems, Int. J. Electr. Power Energy Syst. 134 (2022) 107480.
[42] A. Khergade, R. Satputaley, S.K. Patro, Investigation of voltage sags effects on ASD and mitigation using ESRF theory-based DVR, IEEE Trans. Power Deliv. 36 (6) (2021) 3752–3764.
[43] S. Biricik, et al., Protection of sensitive loads using sliding mode controlled three-phase DVR with adaptive notch filter, IEEE Trans. Ind. Electron. 66 (7) (2018) 5465–5475.
[44] D. Patel, A.K. Goswami, S.K. Singh, Voltage sag mitigation in an Indian distribution system using dynamic voltage restorer, Int. J. Electr. Power Energy Syst. 71 (2015) 231–241.
[45] R. Singh, M. Kumar, H. Ashfaq, An integrated solar photovoltaic and dynamic voltage restorer for load voltage compensation, Int. J. Electr. Eng. Technol. (IJEET) 9 (5) (2018) 52–63.
[46] P. Gambôa, et al., Input–Output Linearization and PI controllers for AC–AC matrix converter based Dynamic Voltage Restorers with Flywheel Energy Storage: a comparison, Electr. Power Syst. Res. 169 (2019) 214–228.
[47] R. Pal, S. Gupta, Topologies and control strategies implicated in dynamic voltage restorer (DVR) for power quality improvement, Iran. J. Sci. Technol., Trans. Electr. Electron. Eng. 44 (2) (2020) 581–603.
[48] M. Farhadi-Kangarlu, E. Babaei, F. Blaabjerg, A comprehensive review of dynamic voltage restorers, Int. J. Electr. Power Energy Syst. 92 (2017) 136–155.
[49] J. Zhang, L. Li, D.G. Dorrell, Control and applications of direct matrix converters: a review, Chin. J. Electr. Eng. 4 (2) (2018) 18–27.
[50] O. Aydogmus, G. Boztas, R. Celikel, Design and analysis of a flywheel energy storage system fed by matrix converter as a dynamic voltage restorer, Energy 238 (2022) 121687.
[51] M. Diaz, et al., An overview of applications of the modular multilevel matrix converter, Energies. (Basel) 13 (21) (2020) 5546.
[52] A. Bento, et al., On the Potential Contributions of Matrix Converters for the Future Grid Operation, Sustainable Transportation and Electrical Drives Innovation, Appl. Sci. 11 (10) (2021) 4597.
[53] J. Van Gorp, M. Caussy, C. Gillot, Binary signals design to control the matrix converter in the context of smart grids, IFAC-PapersOnLine 50 (1) (2017) 2119–2124.
[54] Z. Malekjamshidi, et al., Bidirectional power flow control with stability analysis of the matrix converter for microgrid applications, Int. J. Electr. Power Energy Syst. 110 (2019) 725–736.
[55] L.R. Merchan-Villalba, et al., Linearly decoupled control of a dynamic voltage restorer without energy storage, Mathematics 8 (10) (2020) 1794.
[56] P.W. Wheeler, et al., Matrix converters: a technology review, IEEE Trans. Ind. Electron. 49 (2) (2002) 276–288.
[57] O. Simon, et al., Modern solutions for industrial matrix-converter applications, IEEE Trans. Ind. Electron. 49 (2) (2002) 401–406.
[58] P. Wheeler, et al., A review of multi-level matrix converter topologies, in: 2008 4th IET Conference on Power Electronics, Machines and Drives, IET, 2008.
[59] Z. Idris, S.M. Noor, M.K. Hamzah, Safe commutation strategy in single phase matrix converter, in: 2005 International Conference on Power Electronics and Drives Systems, IEEE, 2005.
[60] P.W. Wheeler, et al., Matrix converters, EEE Ind. Appl. Mag. 10 (1) (2004) 59–65.
[61] J.M. Lozano, J.M. Ramirez, R.E. Correa, A novel dynamic voltage restorer based on matrix converters. 2010 Modern Electric Power Systems, IEEE, 2010.
[62] M. Imayavaramban, A.K. Chaithanya, B. Fernandes, Analysis and mathematical modelling of matrix converter for adjustable speed AC drives, in: 2006 IEEE PES Power Systems Conference and Exposition, IEEE, 2006.
[63] K.B. Tawfiq, et al., Mathematical Modelling, Analysis and Control of a Three to Five-Phase Matrix Converter for Minimal Switching Losses, Mathematics 9 (1) (2021) 96.
[64] A. Tsoupos, V. Khadkikar, A novel SVM technique with enhanced output voltage quality for indirect matrix converters, IEEE Trans. Ind. Electron. 66 (2) (2018) 832–841.
[65] D. Casadei, et al., Matrix converter modulation strategies: a new general approach based on space-vector representation of the switch state, IEEE Trans. Ind. Electron. 49 (2) (2002) 370–381.
[66] M. Faisal, et al., PI controller and park's transformation based control of dynamic voltage restorer for voltage sag minimization, in: 2014 9th International Forum on Strategic Technology (IFOST), IEEE, 2014.
[67] A.H. Soomro, et al., Simulation based Analysis of Single Unit and Parallel Connected Three Phase AC Generator in QUEST Campus Larkana, Sukkur IBA Int. J. Emerg. Technol. 5 (2) (2022) 33–41.
[68] A. Andang, et al., Three-phase Four-leg Inverter LC Filter Using FCS MPC, in: 2021 International Conference on Smart-Green Technology in Electrical and Information Systems (ICSGTEIS), IEEE, 2021.
[69] V. Maniezzo, L.M. Gambardella, F. De Luigi, Ant colony optimization. New Optimization Techniques in Engineering, Springer, 2004, pp. 101–121.
[70] Y.-T. Hsiao, C.-L. Chuang, C.-C. Chien, Ant colony optimization for designing of PID controllers, in: 2004 IEEE International Conference on Robotics and Automation (IEEE Cat. No. 04CH37508), IEEE, 2004.
[71] M. Dorigo, M. Birattari, T. Stutzle, Ant colony optimization, IEEe Comput. Intell. Mag. 1 (4) (2006) 28–39.
[72] H.-b. Duan, D.-b. Wang, X.-f. Yu, Novel approach to nonlinear PID parameter optimization using ant colony optimization algorithm, J. Bionic. Eng. 3 (2) (2006) 73–78.
[73] T. Stützle, et al., Parameter adaptation in ant colony optimization. Autonomous Search, 2011, pp. 191–215.
[74] T. Liao, et al., A unified ant colony optimization algorithm for continuous optimization, Eur. J. Oper. Res. 234 (3) (2014) 597–609.
[75] M.M. Kabir, M. Shahjahan, K. Murase, A new hybrid ant colony optimization algorithm for feature selection, Expert. Syst. Appl. 39 (3) (2012) 3747–3763.
[76] S. Pothiya, I. Ngamroo, W. Kongprawechnon, Ant colony optimisation for economic dispatch problem with non-smooth cost functions, Int. J. Electr. Power Energy Syst. 32 (5) (2010) 478–487.
[77] W.E. Reid, Power quality issues-standards and guidelines, IEEe Trans. Ind. Appl. 32 (3) (1996) 625–632.